Energy Levels and Transition Rates for Laser Cooling Os^- and a General Approach to Produce Cold Atoms and Molecules

Yuzhu Lu(陆禹竹)[1], Rui Zhang(张瑞)[1], Changxian Song(宋昌仙)[2], Chongyang Chen(陈重阳)[2], Ran Si(司然)[2*], and Chuangang Ning(宁传刚)[1,3*]

[1]*Department of Physics, State Key Laboratory of Low-Dimensional Quantum Physics, Tsinghua University, Beijing 100084, China*

[2]*Shanghai EBIT Lab, Key Laboratory of Nuclear Physics and Ion-Beam Application (MOE), Institute of Modern Physics, Department of Nuclear Science and Technology, Fudan University, Shanghai 200433, China*

[3]*Frontier Science Center for Quantum Information, Tsinghua University, Beijing 100084, China*

(Received 25 May 2023; accepted manuscript online 16 August 2023)

High-resolution photoelectron energy spectra of osmium anions are obtained using the slow-electron velocity-map imaging method. The energy levels of excited states $^4F_{7/2}$, $^4F_{5/2}$ and $^4F_{3/2}$ of Os^- are determined to be 148.730(13), 155.69(15), and 176.76(13) THz [or 4961.09(41), 5193.4(49), and 5896.1(42) cm^{-1}], respectively. The lifetime of the opposite-parity excited state $^6D^o_{9/2}$ is determined to be 201(10) μs using a cold ion trap, about 15 times shorter than the previous result 3(1) ms. Our high-level multi-configuration Dirac–Hartree–Fock calculations yield a theoretical lifetime 527 μs. Our work shows that the laser cooling rate of Os^- is as fast as that of Th^-. The advantages of Os^- are its near-IR range cooling transition and simple electronic structure, which make Os^- a promising candidate for laser cooling of negative ions. We propose a general approach to produce cold atoms and molecules based on the sympathetic cooling of negative ions in combination with a threshold photodetachment.

DOI: 10.1088/0256-307X/40/9/093101

Osmium (Os, $Z = 76$) is known as the densest element in nature, and also the rarest precious metal. The anion of Os has drawn continuous interest of both experimental[1–6] and theoretical studies[7,8] due to its potential in laser cooling. As is well known, laser cooling is the key to ultracold physics, and it has been successfully applied to neutral and positive atoms and molecules.[9–13] However, laser cooling of negative ions has never been achieved. Due to the relatively weak and short-range interaction between the extra electron and the neutral core, most anions have few bound states. Consequently, a fast bound-bound electric dipole ($E1$) transition, which is required for laser cooling, is rare for anions.[1–8,14–23] Up to date, only Os^-,[1,3,15] Ce^-,[16,17] La^-,[18–21] and Th^- [22,23] were experimentally confirmed to have opposite-parity bound states. Os^- is the first anion discovered to have a bound $E1$ transition,[1] and the feasibility for laser cooling Os^- has been investigated.[3,5,8,15] The ground state of Os^- is $5d^76s^2\,^4F^e_{9/2}$ with an even parity. Theoretical calculations suggested that the shallowly bounded state of Os^- observed by Bilodeau and Haugen was $5d^76s^26p^6D^o_{9/2}$ and its parity was odd.[7] The transition frequency of Os^- $^4F^e_{9/2} \rightarrow {}^6D^o_{9/2}$ was measured to be 257.831190(35) THz or 8600.3227(12) cm^{-1}.[3] The hyperfine structure[15] and the Zeeman splitting[5] of the two related states were also experimentally measured. However, the candidate laser cooling transition $^4F^e_{9/2} \rightarrow {}^6D^o_{9/2}$ was very slow according to the experiment of Warring *et al.* They deduced that the radiation lifetime of the Os^- $^6D^o_{9/2}$ state was 3(1) ms via the saturated resonant absorption.[3] This rather slow cooling transition nearly made Os^- a hopeless candidate for laser cooling.

In this Letter, we report the high-resolution photoelectron energy spectra of osmium anion and lifetime of the Os^- $^6D^o_{9/2}$ state. The radiation lifetime of the $^6D^o_{9/2}$ state was found to be more than 10-fold shorter than the previous results. The main obstacle to laser cooling Os^- has been cleared. The wavelength of the cooling transition of Os^- ($\lambda = 1162.75$ nm) is in the near-IR range. A laser and optical devices are more readily available in this range than those in the mid-IR range for La^- and Th^-.[19,23] In addition, the electronic structure of Os^- is simpler than that of La^- and Th^-. Thus, Os^- is also a promising candidate for the laser cooling of negative ions. In principle, once one kind of negative ions is laser-cooled, other negative ions can be sympathetically cooled by confining them together in one trap. Compared with the laser cooling of positive ions, a distinctive feature of negative ions is that the extra electron can be effectively photodetached by laser radiation. Since the electron mass m_e is much less than the mass of the neutral atom or molecule (M), the kinetic energy of the neutral atom or molecule is much less than that of the photoelectron E_k after photodetachment. For example, if $E_k = 1$ meV and $M = 100$ u, the kinetic energy of the neutral atom or molecule after photodetachment is $(m_e/M)E_k = 5.5$ neV, which corre-

*Corresponding authors. Email: rsi@fudan.edu.cn; ningcg@tsinghua.edu.cn

© 2023 Chinese Physical Society and IOP Publishing Ltd

sponds to a temperature $\sim 60\,\mu$K. Therefore, the laser cooling of anions not only creates a new quantum system but also provides a general approach to producing cold atoms and molecules through sympathetic cooling in combination with threshold photodetachment. During the last decade, there has been a major effort to extend laser cooling techniques from atoms to molecules, which mainly relies on the following two methods: (1) preparing cold molecules via magnetic-photo association of laser-cooled atoms, such as KRb,[24] which is limited to the formation of alkali metal dimers and one trimer;[25,26] (2) directly laser cooling molecules. The challenge of laser cooling a molecule is that there are many branches requiring repumping lasers to close the optical cycling due to its vibrational and rotational freedoms. A molecule having a transition with quasi-diagonal Franck–Condon factors can reduce the number of repumping laser. Several molecules have been directly laser cooled, such as SrF,[27] CaF,[28,29] YO,[30] SrOH,[31] CaOH,[32] and $CaOCH_3$.[33] A few species have been cooled via deceleration and trapping of molecules in a molecular beam.[25,34,35] The aforementioned cooling methods rely on particular properties of a molecule, and therefore are limited to specific species. However, most atoms and molecules can form negative ions.[36] The negatively charged species can be sympathetically cooled by the laser-cooled anions. The corresponding cold neutral species can be produced via a threshold photodetachment, and loaded into a magneto-optical trap or other type of traps. Therefore, the realization of laser cooling negative ions can greatly extend the scope of cold atoms and molecules, such as the cold Cl atoms of chemical interest and the cold ThO molecules for the electron electric dipole moment measurement.[37]

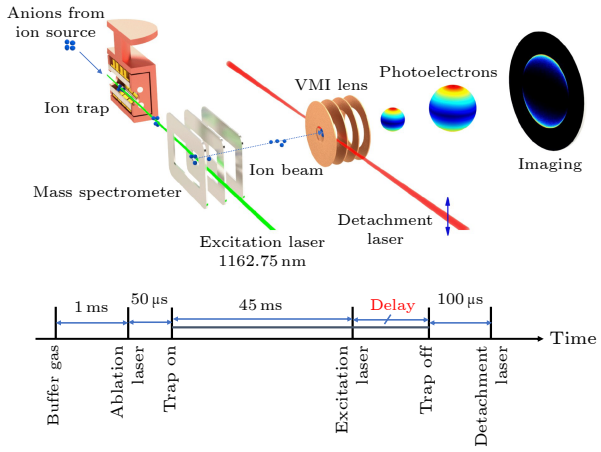

Fig. 1. Schematic view of our cryo-SEVI apparatus and the time sequence for the excited state's lifetime measurement by adjusting the delay between the excitation laser pulse and the trap-off pulse.

Methods and Results. The successful application of laser cooling Os^- requires a precise understanding of the energy levels and the transitions between the upper state $^6D^o_{9/2}$ and the ground state $^4F_{9/2}$. We use the slow-electron velocity-map imaging (SEVI) method to measure the energy levels of Os^-. Our SEVI spectrometer has been introduced before.[38,39] Briefly, the spectrometer consists of the laser ablation ion source, a cryogenically controlled ion trap (5–300 K), a Wiley–McLaren type time-of-flight (TOF) mass spectrometer, and a photoelectron velocity-map imaging (VMI) system, as shown in Fig. 1. The Os^- anions were generated by ablation of an osmium metal disk using a pulsed Nd:YAG laser. The produced anions were captured by the ion trap, and cooled through collisions with the buffer gas. The buffer gas (He or H_2) was delivered into the trap via a pulsed valve 1 ms in advance. Anions were stored in the trap for ~ 45 ms before being ejected to the TOF mass spectrometer. Os^- anions were selected out by a mass gate, and photodetached by a tunable laser. To measure the energy levels of Os^-, a tunable dye laser (400–920 nm and linewidth 0.06 cm^{-1} (0.0018 THz) at 625 nm) pumped by a Quanta-Ray Pro 290 Nd:YAG laser (20 Hz and 1000 mJ/pulse at 1064 nm) was used. The photon energy was further monitored by a wavelength meter (HighFinesse WS6-600) with an accuracy of 0.02 cm^{-1} (0.0006 THz). A charge-coupled-device camera recorded the position of outgoing photoelectrons which were projected on a phosphor screen behind a set of microchannel plates. The spherical shell of photoelectrons exhibited a cylindrical symmetry. The 3D distribution of photoelectrons was reconstructed from the projected 2D images via the maximum entropy velocity Legendre reconstruction method.[40,41] To measure the lifetime of the Os^- $^6D^o_{9/2}$ state, the 1162.75-nm output of an optical parametric oscillator (OPO) was directed through the ion trap to excite Os^- anions from the ground $^4F_{9/2}$ state to the $^6D^o_{9/2}$ state. The laser system operates at a repetition rate of 20 Hz.

Figure 2 shows the photoelectron energy spectra acquired at different wavelengths and the assignment of peaks. The assignment is based on the selection rules of photodetachment, the well-known energy levels of the neutral Os atom, and theoretical calculations. Peaks h, i, k, and l correspond to photodetachment channels from the ground state $^4F_{9/2}$ of Os^-. To observe the excited states with short survival times in the trap due to either collisions or spontaneous radiations, the ion trap can be turned off. When the ion trap was turned off, anions flew directly through the trap and the time of flight of Os^- anions from the ion source to the photodetachment zone is around 150 µs. Extra peaks a–g were observed in this mode, which were assigned to three excited states of Os^-. Peaks c, f, and j belong to the Os^- $^4F_{7/2}$ state; peaks b and e belong to the Os^- $^4F_{5/2}$ state; peaks a, d, and g belong to the Os^- $^4F_{3/2}$ state. The laser cooling transition Os^- $^4F_{9/2} \leftrightarrow {}^6D^o_{9/2}$ has been accurately measured as 8600.3227(12) cm^{-1} (257.831190(35) THz) by Warring *et al.*[3] Since transition Os^- $^4F_{7/2} \leftrightarrow {}^6D^o_{9/2}$ is an $E1$ transition, $^6D^o_{9/2}$ should have a significant branch decaying into $^4F_{7/2}$, which is a long-lifetime state requiring a repump laser. To determine its energy level as accurately as possible, we scanned the photon energy of the detachment laser around the thresholds of transitions l and j (see the Supplementary Information). The binding energy of photodetachment transition l [Os^- $^4F_{9/2} \rightarrow Os$ $^5F_5$] was

determined to be 13835.84(19) cm^{-1} (414.7880(57) THz), and 12473.66(36) cm^{-1} (373.951(11) THz) for transition j [$Os^- {}^4F_{7/2} \rightarrow Os\, {}^5F_4$]. Since multiple transitions were observed, a fully correlated analysis of the variances and covariances has been conducted to optimize the energy levels. The obtained results are listed in Table 1 in comparison with our theoretical predictions. We updated the electron affinity of Os as 8691.92(19) cm^{-1} (260.5772(57) THz) or 1.077661(24) eV, instead of 1.07780(12) eV previously reported by Bilodeau and Haugen via the laser photodetachment threshold method.[1] The energy level of $^4F_{7/2}$ was updated as 4961.09(41) cm^{-1} (148.730(13) THz) above the ground state $^4F_{9/2}$. The systematic error was estimated to be 0.04 cm^{-1} (0.0012 THz). The uncertainty includes both statistical and systematic uncertainties. The energy level for $^4F_{7/2}$ reported by Bilodeau and Haugen was 4231(25) cm^{-1} [1] (126.84 (75) THz), significantly deviating from the present result. Since several transitions from $^4F_{7/2}$ (peaks c, f, and j) were observed in the present work, the accurate energy levels of Os can provide the fingerprint-like check for the assignment. We believe that the 4231(25) cm^{-1} (126.84(75) THz) value is likely due to an unknown contamination.

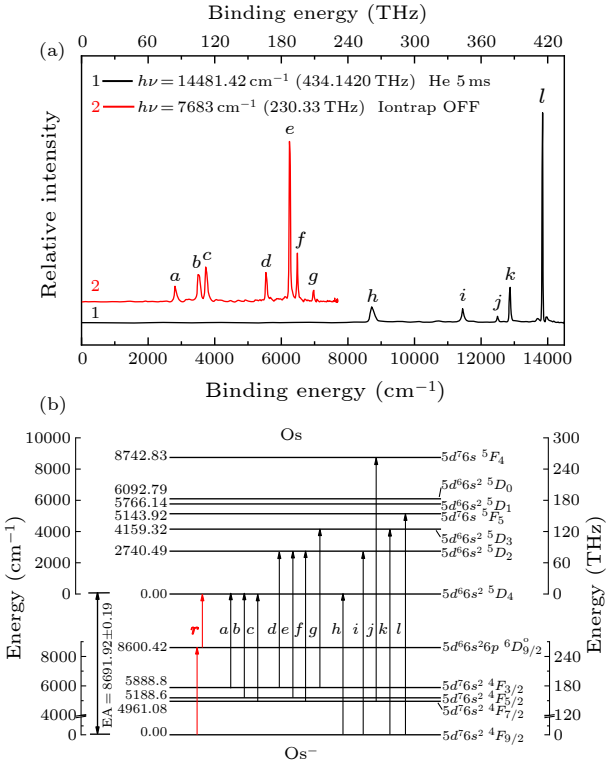

Fig. 2. Photoelectron energy spectra of Os^- collected using the 14481.42 cm^{-1} (434.1420 THz) output of the dye laser (black line, anions were trapped for 5 ms, and buffer gas was He) and the 7683 cm^{-1} (230.33 THz) idler output of OPO (red line, the ion trap was turned off) (a) and the transition assignment for the observed peaks (b). EA: electron affinity.

The $^6D^o_{9/2}$ state was not observed in the photoelectron spectra in Fig. 2 due to its short lifetime. Its binding energy is only 91.50(19) cm^{-1} (2.7431(57) THz) and can be detached by the blackbody radiation from the environment at room temperature. To measure the lifetime of the $^6D^o_{9/2}$ state, we conducted the experiment at a low temperature of 15 K in the ion trap to avoid the detachment from the blackbody radiation and collisions from the residual gas. The loss rate due to the blackbody radiation detachment is estimated to be $\sim 10^{-4}$ per second at 15 K. A laser beam with a wavelength of 1162.75 nm from our OPO laser system was used to resonantly excite Os^- to its $^6D^o_{9/2}$ state in the ion trap. The Os^- anions were cooled in the trap for 45 ms through collisions with the buffer gas (H_2) delivered by a pulsed valve. Then, the 1162.75-nm laser pulse was turned on slightly before the anions were ejected out from the trap. The excited anions flew for approximately 100 μs from the ion trap into the interaction zone of the VMI and were photodetached there by a pulsed 1064-nm laser (see the Supplementary Information). Peak r in Fig. 3(a) is corresponding to the photodetachment channel $Os^- {}^6D^o_{9/2} \rightarrow Os\, {}^5D_4$. The relative intensity of peak r to peak h reveals the relative population of Os^- in its excited state $^6D^o_{9/2}$. As shown in Fig. 4, the intensity ratio of peak r to peak h is plotted versus the delay from the excitation laser pulse to the ejection of trapped anions. The lifetime of the Os^- $^6D^o_{9/2}$ state was determined to be 201(10) μs via an exponential decay fitting. The uncertainty ±10 μs was given via the fitting procedure. The background pressure of the chamber was 5.0×10^{-5} Pa. The buffer gas density in the ion trap was expected to be in dynamic equilibrium with the background after a trapping period of 45 ms. The mean free time between collisions was estimated to be 5 ms, much longer than the lifetime. To experimentally evaluate the collision effect on the lifetime, the pressure was increased to 1.0×10^{-4} Pa and 2.0×10^{-4} Pa, and the lifetime of $^6D^o_{9/2}$ was measured to be 205(14) μs and 180(9) μs, respectively. Thus, the de-excitation due to collisions with the background gas was negligible at 5.0×10^{-5} Pa. The dc and ac fields for trapping anions in our measurement is ~ 1 V/m, while the static electric filed required for the detachment of excited state is $\sim 10^6$ V/m.[3] Consequently, the field detachment during the trapping period is negligible. The systematic error for the lifetime measurement should be small when compared with the statistical error since the time intervals were controlled with a pulse controller with an accuracy of 1 ns, and the effects, such as collisions, black-body radiation, field detachment on the lifetime are negligible. Since no notable signal related to transitions c and f from $^4F_{7/2}$ was observed, we concluded that the excited state $^6D^o_{9/2}$ dominantly decays to the ground state $^4F_{9/2}$ via spontaneous radiation, and the branch ratio to $^4F_{7/2}$ was estimated to be less than 5%.

The measured lifetime (τ = 201(10) μs) of $^6D^o_{9/2}$ is much shorter than the previous experimental result 3(1) ms via measuring the resonant absorption cross section σ_a by Warring *et al.*[3] and the theoretical prediction 3.8 ms by O'Malley and Beck,[7] but consistent with the estimated Einstein coefficient $\sim 10^4\ s^{-1}$ or $10^5\ s^{-1}$ for the resonant transition by Bilodeau and Haugen.[1] It should be pointed out that σ_a tends to be underestimated if the

frequency of the excitation laser deviates from the resonance center. Consequently, the lifetime was overestimated due to the underestimated σ_a.

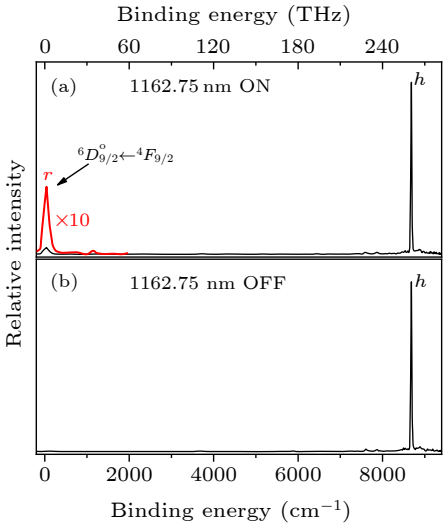

Fig. 3. Photoelectron energy spectra of anions with (a) and without (b) the excitation laser with a wavelength 1162.75 nm. The wavelength of the photodetachment laser is 1064 nm.

To better understand the obtained results and to predict the branch ratio of the optical cycling for laser cooling Os^-, we calculated the bound states of Os^- using the multi-configuration Dirac–Hartree–Fock (MCDHF) method, as implemented in the GRASP package.[42,43] The transverse photon (Breit) interaction and the leading quantum electrodynamic corrections (vacuum polarization and self-energy) were accounted for in the relativistic configuration interaction (RCI) calculations. In the first step, a Dirac–Hartree–Fock calculation was performed for the $5d^76s^2\,{}^4F_{9/2,7/2,5/2,3/2}$ and $5d^66s^26p^6D^o_{9/2}$ levels. These orbitals are kept to be fixed in the following calculations. Then, the configuration-state-function (CSF) expansions were obtained using the restricted-active-set method, by allowing single and double substitutions from the reference configurations, $5d^76s^2$ and $5d^66s^26p$, to the active set space. We defined the $5d$ and $6p$ electrons as valence electrons, the remaining as core electrons. When the substitutions were all from valence electrons, valence-valence (VV) correlation was included; core-valence (CV) correlation was included when we allow at the most single substitution from the core subshells; core-core (CC) correlation could be included when we allow both single and double substitutions from the core subshells, either as intra-CC if only substitutions from one core subshell at one time or inter-CC if substitutions from different core subshells are allowed at one time. The correlation orbitals were further optimized based on VV substitutions in the MCDHF procedure, the active set space was increased up to $9s9p9d9f8g7h$ (AS9) systematically by adding layers of orbitals, i.e., a set of virtual orbitals specified by its principal quantum number. The MCDHF calculation was followed by RCI calculations for an extended expansion, where CV, intra-CC, and inter-CC correlations due to the $6s$, $5p$, and $5s$ subshells were included. The numbers of CSFs in the final even and odd state expansions, accounting for VV, CV and CC electron correlations, were 3026363 and 7778018, respectively, distributed over the different J symmetries.

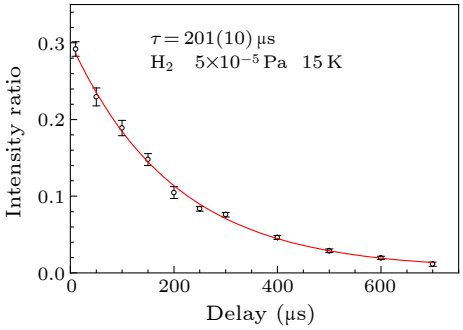

Fig. 4. The intensity ratio of peak r to peak h versus the delay between the excitation laser pulse and the ejection of anions. The solid line is the fitting curve according to the equation $I(t) = I_0 e^{-t/\tau}$.

Table 1. Measured and calculated excitation energies of Os^- states (in cm^{-1}). The values in THz are listed in the brackets. The energies are relative to the ground state $^4F_{9/2}$.

State	Measured (this work)	Measured (other work)	Calculated (this work)
$^4F_{9/2}$	0	0	0
$^4F_{7/2}$	4961.09(41) [148.730(13)]	4231(25)[a] [126.84(75)]	4816 [144.4]
$^4F_{5/2}$	5193.4(49) [155.69(15)]		6373 [191.1]
$^4F_{3/2}$	5896.1(42) [176.76(13)]		6856 [205.5]
$^6D^o_{9/2}$		8600.3227(12)[b] [257.831190(35)]	8645 [259.2]

[a]From Ref. [1]. [b]From Ref. [3].

Table 1 presents the calculated energy levels of the bound states of Os^- in comparison with the experimental results. It can be seen that the predicted values of $^4F_{7/2}$ and $^6D^o_{9/2}$ agree well with the measured values, while the agreement is not so satisfactory for $^4F_{5/2}$ and $^4F_{3/2}$. Table 2 lists the lifetimes and branching ratios of excited states of Os^-. The calculated lifetime for $^6D^o_{9/2}$ is 527 µs, almost one order of magnitude shorter than the previous prediction 3.8 ms by O'Malley and Beck.[7] The present calculation improves the agreement with the present measurement, but it is still 2.6 times longer than the experimental value 201(10) µs. The lifetime of $^6D^o_{9/2}$ is dominated by two inter-combination $E1$ transitions to $^4F_{9/2,7/2}$. These inter-combination lines are spin-induced transitions

by relativistic spin-dependent effects, thus are very sensitive to electron correlation and remain as a difficult task for theoretical studies. To investigate the discrepancies between our calculated lifetime and that reported by O'Malley and Beck,[7] we performed a test calculation on the $E1$ transitions, in which only the VV and CC_{6s} correlations were included, similar to the calculation strategy in Refs. [7,8]. We obtained a lifetime 4.07 ms, in good agreement with the result from Ref. [7], which illustrates that the differences between our final MCDHF + RCI calculations and those of O'Malley and Beck are mainly due to the CV and CC effects from inner core subshells, and highlights the importance of opening up more inner cores.

Table 2. Theoretical lifetimes (τ) and transition wavelengths (λ) in nm, transition rates (A) in s^{-1} of excited states of Os^-. Numbers in brackets represent powers of 10. Branching ratios are 100%, except for $^6D^o_{9/2} \rightarrow {}^4F_{9/2}$ (99.6%) and $^6D^o_{9/2} \rightarrow {}^4F_{7/2}$ (0.4%).

Levels	Type	λ	A	τ (this work)	τ (Ref. [7])
$^4F_{7/2} \rightarrow {}^4F_{9/2}$	$M1$	2076	3.50[+0]	285 ms	420 ms
$^4F_{5/2} \rightarrow {}^4F_{7/2}$	$M1$	6423	1.69[−1]	5.91 s	4.2 s
$^4F_{3/2} \rightarrow {}^4F_{5/2}$	$M1$	20686	3.29[−3]	304 s	230 s
$^6D^o_{9/2} \rightarrow {}^4F_{9/2}$	$E1$	1 157	1.89[+3]	527 µs	3.8 ms
$\rightarrow {}^4F_{7/2}$	$E1$	2 612	8.15[+0]		

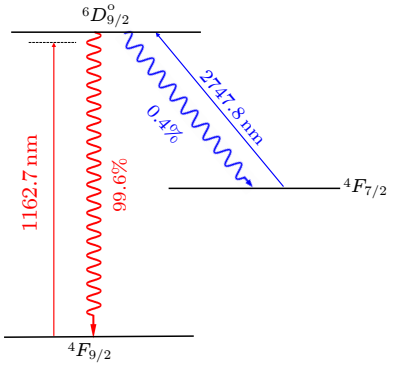

Fig. 5. Optical cycling for the laser cooling of Os^-. The percentage is the theoretical branch ratio.

The nuclear spin of ^{192}Os (the most abundant isotope, 41%) is 0. Therefore, there is no hyperfine splitting of the transitions, which greatly simplifies the laser system required for laser cooling. Figure 5 shows the optical cycling for laser cooling Os^-. The laser at wavelength 2747.8 nm is employed to repump Os^- from the intermediate state $^4F_{7/2}$ to $^6D^o_{9/2}$. Based on the new lifetime, the natural width for the transition $^6D^o_{9/2} \leftrightarrow {}^4F_{9/2}$ is 0.80 kHz, and the minimum temperature achievable with Doppler cooling is $T_D = 19$ nK. Since the cooling transition rate is relatively low ($5 \times 10^3\,s^{-1}$), it is impractical to initiate cooling directly from room temperature using laser cooling. It is better to precool Os^- anions to a temperature of a few K via buffer gas cooling, and then cool them further down to T_D via laser cooling. It requires scattering 2×10^4 photons from 10 K to T_D and hence takes 8.1 s if in saturation, which is almost as fast as the laser cooling of Th^- ($t = 7.8$ s).[22,23] The photodetachment loss of negative ions at their excited state during the laser-cooling period is another factor to consider. Fortunately, this loss is usually insignificant if a narrow-linewidth cooling laser is used. For the laser cooling of Os^-, the photodetachment cross section of $^6D^o_{9/2}$ at $\lambda = 1162.7$ nm is approximately $5 \times 10^{-21}\,m^2$ as experimentally estimated by Bilodeau and Haugen.[1] If a cooling laser with a linewidth of 0.80 kHz is utilized and the saturation parameter $s = 2$, the photodetachment loss during the laser-cooling period ($t = 12.2$ s when $s = 2$) is 0.03%, which is negligible. The cost of a laser with sub-kHz linewidth is relatively high. However, if a cooling laser with a linewidth of 100 kHz, a typical linewidth of an external-cavity diode laser, is utilized, the loss rate will be 4%, which is still acceptable. With a sideband cooling in an ion trap, once the ion is cooled into the vibrational ground state, it will no longer absorb light since it is well off resonance, so there will be no further photodetachment loss although the cooling laser may be still on.

In summary, we have measured the energy levels of Os^- and the lifetime of its excited state $^6D^o_{9/2}$. Our experimental results demonstrate that the transition rate for laser cooling is an order of magnitude faster than the previously measured value. This finding suggests that Os^- represents a promising candidate for laser cooling negative ions. Compared with the candidate Th^-, the advantage of Os^- is that the laser cooling transition is in the near-IR range. Lasers and optical devices in this range are available at a much lower cost than that in the mid-IR band ($\lambda = 2428.4$ nm for Th^-). Moreover, the electronic structure of Os^- is less complex, with all energy levels having been measured, whereas only partial states of Th^- have been observed. We are planning the experiments for laser cooling Os^- and Th^- in the future. The success of laser cooling negative ions will not only create a new quantum system but also provide a general method for producing cold atoms and molecules.

Acknowledgments. This work was supported by the National Natural Science Foundation of China (Grant No. 11974199), the National Key R&D Program of China (Grant No. 2018YFA0306504), and the Innovation Program for Quantum Science and Technology (Grant No. 2021ZD0301602).

References

[1] Bilodeau R C and Haugen H K 2000 *Phys. Rev. Lett.* **85** 534

[2] Warring U, Canali C, Fischer A *et al.* 2009 *J. Phys.: Conf. Ser.* **194** 152022

[3] Warring U, Amoretti M, Canali C *et al.* 2009 *Phys. Rev. Lett.* **102** 043001
[4] Kellerbauer A and Fritzsche S 2012 *J. Phys.: Conf. Ser.* **388** 012023
[5] Kellerbauer A, Fischer A, and Warring U 2014 *Phys. Rev. A* **89** 043430
[6] Kellerbauer A, Canali C, Fischer A *et al.* 2011 *Phys. Rev. A* **84** 062510
[7] O'Malley S M and Beck D R 2010 *Phys. Rev. A* **81** 032503
[8] Pan L and Beck D R 2010 *Phys. Rev. A* **82** 014501
[9] Shi Z L, Li Z L, Wang P J *et al.* 2018 *Chin. Phys. Lett.* **35** 123701
[10] Zhang J, Deng K, Luo J *et al.* 2017 *Chin. Phys. Lett.* **34** 050601
[11] Chen T, Du L J, Song H F *et al.* 2015 *Chin. Phys. Lett.* **32** 083701
[12] Wang S G, Zhang J W, Miao K *et al.* 2013 *Chin. Phys. Lett.* **30** 013703
[13] Wang B, Lü D S, Qu Q Z *et al.* 2011 *Chin. Phys. Lett.* **28** 063701
[14] Yzombard P, Hamamda M, Gerber S *et al.* 2015 *Phys. Rev. Lett.* **114** 213001
[15] Fischer A, Canali C, Warring U *et al.* 2010 *Phys. Rev. Lett.* **104** 073004
[16] Walter C W, Gibson N D, Janczak C M *et al.* 2007 *Phys. Rev. A* **76** 052702
[17] Walter C W, Gibson N D, Li Y G *et al.* 2011 *Phys. Rev. A* **84** 032514
[18] Walter C W, Gibson N D, Matyas D J *et al.* 2014 *Phys. Rev. Lett.* **113** 063001
[19] Cerchiari G, Kellerbauer A, Safronova M S *et al.* 2018 *Phys. Rev. Lett.* **120** 133205
[20] Jordan E, Cerchiari G, Fritzsche S *et al.* 2015 *Phys. Rev. Lett.* **115** 113001
[21] Kellerbauer A, Cerchiari G, Jordan E *et al.* 2015 *Phys. Scr.* **90** 054014
[22] Tang R L, Si R, Fei Z J *et al.* 2019 *Phys. Rev. Lett.* **123** 203002
[23] Tang R L, Si R, Fei Z J *et al.* 2021 *Phys. Rev. A* **103** 042817
[24] Ni K K, Ospelkaus S, de Miranda M H G *et al.* 2008 *Science* **322** 231
[25] Krems R, Friedrich B, and Stwalley W C 2009 *Cold Molecules: Theory, Experiment, Applications* (Boca Raton: CRC Press)
[26] Yang H *et al.* 2022 *Science* **378** 1009
[27] Barry J F, Shuman E S, Norrgard E B *et al.* 2012 *Phys. Rev. Lett.* **108** 103002
[28] Anderegg L, Augenbraun B L, Chae E *et al.* 2017 *Phys. Rev. Lett.* **119** 103201
[29] Anderegg L, Burchesky S, Bao Y *et al.* 2021 *Science* **373** 779
[30] Ding S Q, Wu Y W, Finneran I A, Burau J J, and Ye J 2020 *Phys. Rev. X* **10** 021049
[31] Kozyryev I *et al.* 2017 *Phys. Rev. Lett.* **118** 173201
[32] Vilas N B, Hallas C, Anderegg L *et al.* 2022 *Nature* **606** 70
[33] Mitra D, Vilas N B, Hallas C *et al.* 2020 *Science* **369** 1366
[34] Prehn A, Ibrügger M, Glöckner R *et al.* 2016 *Phys. Rev. Lett.* **116** 063005
[35] Cheng C F, van der Poel Aernout P P, Jansen P *et al.* 2016 *Phys. Rev. Lett.* **117** 253201
[36] Ning C G and Lu Y Z 2022 *J. Phys. Chem. Ref. Data* **51** 021502
[37] Baron J, Campbell W C, DeMille D *et al.* 2014 *Science* **343** 269
[38] Luo Z H, Chen X L, Li J M *et al.* 2016 *Phys. Rev. A* **93** 020501
[39] Tang R L, Fu X X, and Ning C G 2018 *J. Chem. Phys.* **149** 134304
[40] Dick B 2014 *Phys. Chem. Chem. Phys.* **16** 570
[41] Dick B 2019 *Phys. Chem. Chem. Phys.* **21** 19499
[42] Fischer C F, Godefroid M, Brage T *et al.* 2016 *J. Phys. B: At. Mol. Opt. Phys.* **49** 182004
[43] Froese F C, Gaigalas G, Jönsson P *et al.* 2019 *Comput. Phys. Commun.* **237** 184